Electronic Supplementary Information for

Thermally activated polymorphic transition from 1D ribbon to 2D carpet: squaric acid on Au(111)

Kan Ueji,‡[ab] Jaehoon Jung,‡[a] Junepyo Oh,[a] Kazuo Miyamura[b] and Yousoo Kim*[a]

[a] Surface and Interface Science Laboratory, RIKEN, 2-1 Hirosawa, Wako, Saitama 351-0198, Japan.
Fax: +81 48 467 1945; Tel: +81 48 467 4073; E-mail: ykim@riken.jp
[b] Department of Chemistry, Faculty of Science, Tokyo University of Science,
1-3 Kagurazaka, Shinjuku, Tokyo 162-8601, Japan.
‡ These authors contributed equally to this work

Figure S1. (a) Large-scale STM images (240 × 240 nm^2) of 1D ribbon superstructure formed on Au(111) [V_s = 100 mV, I_t = 0.5 nA (left); V_s = 100 mV, I_t = 0.3 nA (right)], and (b) the histograms of measured ribbon widths for the relatively low (top, *ca.* 0.15 ML) and the high (bottom, *ca.* 0.23 ML) surface coverages. In order to plot the histogram, we measured the width of the 65 and 69 ribbon structures for the deposition of 0.15 and 0.23 ML, respectively.

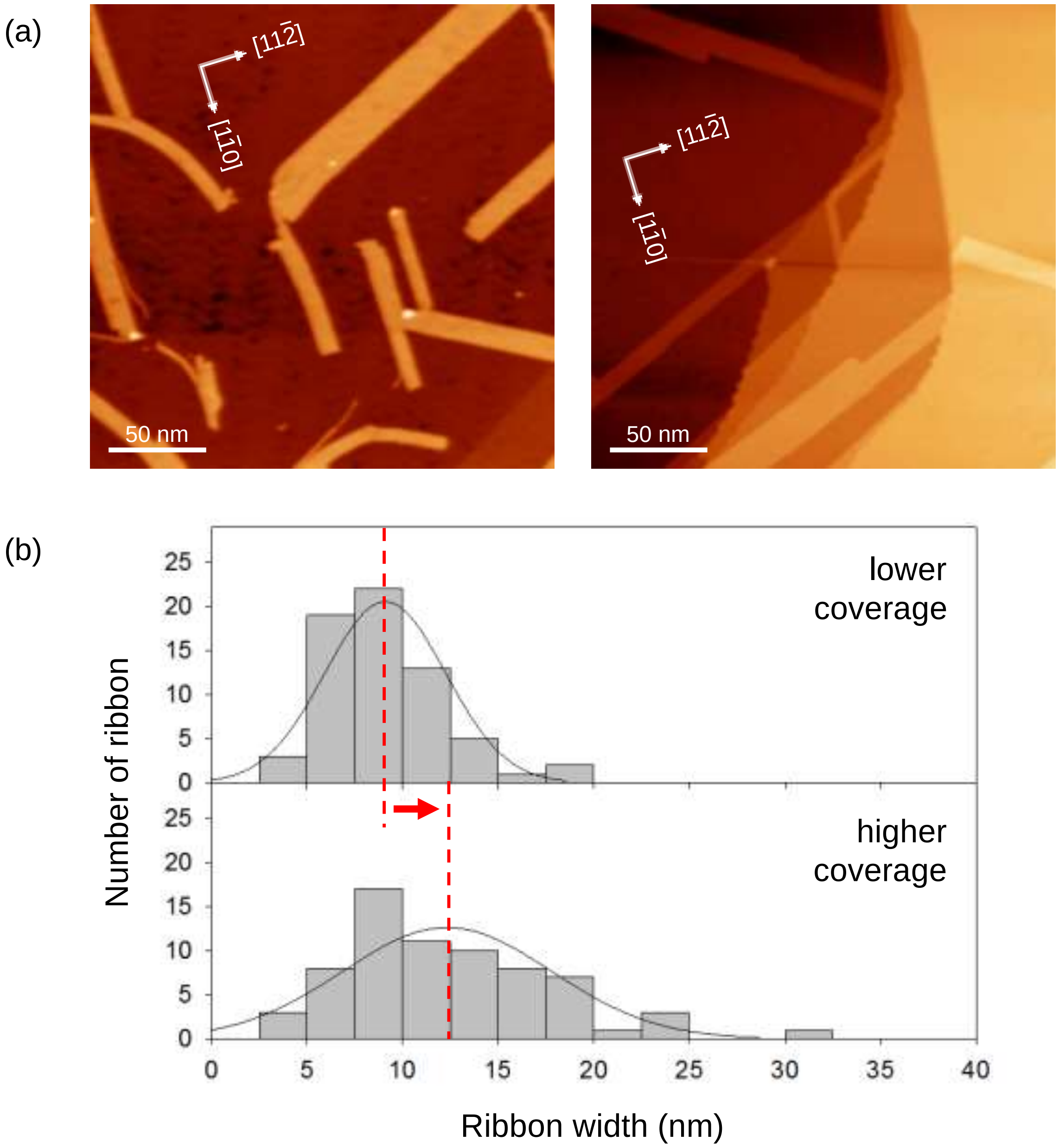

Table S1. Unit cell parameters of the 1D ribbon and 2D carpet H_2SQ superstructures obtained from STM experiments and DFT-D2 (implemented in VASP) calculations (see Figures 2 and 3 in the main manuscript).

	a	b	γ	Area/molecule
1D ribbon superstructure				
STM Exp.	6.4±0.3 Å	11.6±0.4 Å	82±0.1°	36.76±3.01 Å/molecule
DFT-D2	6.13 Å	11.23 Å	82.0°	34.08 Å/molecule
2D carpet superstructure				
STM Exp.	6.2±0.2 Å	6.2±0.2 Å	90°	38.44±2.48 Å/molecule
DFT-D2	5.98 Å	5.98 Å	90.0°	35.76 Å/molecule

Computation details

We performed extensive periodic density functional theory (DFT) calculations with a variety of molecular arrangements to interpret our experimental observations using scanning tunneling microscopy (STM). We employed the DFT-D2 method[S1] implemented in the Vienna Ab initio Simulation Package (VASP) code[S2] in order to take into account van der Waals forces. Core electrons were replaced by projector augmented wave (PAW) pseudopotentials,[S3] expanded in a basis set of plane waves up to a cut-off energy of 400 eV. The squaric acid (H_2SQ, see Scheme 1 in the main manuscript) molecule has five geometric isomers depending on the position of the hydrogen atoms;[S4] thus, we first optimized isolated H_2SQ isomers using a cubic box with side lengths of 20 Å in order to construct initial geometries for the periodic molecular configurations (Table S2). The calculated relative energies are reported in the first column of Table S2, which were compared with other computational results obtained by a variety of DFT methods using the Gaussian09 (G09) software package.[S5] Although the stability order of isomers **c** and **d** changes depending on the level of DFT methodology, all DFT methods provide a good agreement for the much higher stability of isomers **a** and **b**, i.e., the **ZZ** and **EZ** isomers discussed in the main manuscript. (See the webpage, http://www.gaussian.com/g_tech/g_ur/k_dft.htm, for detailed descriptions of the employed DFT methods.) Therefore, our choice of DFT-D2 provides sufficient accuracy in describing the relative stability among the H_2SQ isomers at the single-molecule level, and further in application to calculate the periodic molecular configurations.

Figures S2-S4 show the initial molecular configurations composed of each of the five isomers in order for the optimization procedure to obtain both one-dimensional (1D) ribbon and 2D carpet H_2SQ superstructures, as observed in our STM experiments (see Figures 1 and 2 in the main manuscript). Because the measured widths of 1D ribbon superstructures are quite large (see Figure 2 in the main manuscript), we only considered 2D periodic configurations in the calculations. Based on the experimentally observed molecular arrangement for the ribbon superstructure, we constructed the initial supercells including two H_2SQ molecules. Also, we considered three types of molecular arrangements for the initial molecular configurations: (1) a rectangular grid arrangement, as shown in Figure S2, in which the four-membered carbon rings of the H_2SQ molecules were positioned parallel to the unit vectors of the supercell, and the closest distance between the centers of the four-membered carbon rings was set to 6 Å; (2) a rectangular grid arrangement with the molecules rotated from (1) by anticlockwise 25°, as shown in Figure S3; and (3) a parallelogrammic arrangement tilted from rectangular (1) by ±7°, as shown in Figure S4. For each arrangement, 12 molecular configurations composed of H_2SQ isomers were considered. During ionic relaxation, the molecular geometry was maintained as planar by symmetry constraints, but the volume and shape of the slab were freely adjusted toward a local potential minimum. To ensure 2D molecular architectures, we initially separated the periodically replicated slabs with a large vacuum region of 25 Å. The resultant vacuum regions of the optimized slabs ranged 6.0–7.8 Å, in which the interaction between molecular layers is expected to be insignificant in obtaining proper geometries and energies of H_2SQ superstructures. The convergence threshold was set to 10^{-7} eV in energy and 0.01 eV/Å in atomic forces. A 2×4×1 Γ-centered grid was used for the k-point sampling of first Brillouin zone. The binding energy was evaluated with respect to the energy of the most stable isomer **a** (Table S1) in the gas phase, regardless of the isomer species in the optimized periodic molecular configurations. Finally, Figure S5 shows the eight stable superstructures which have relative energies within 10 kcal/mol per one H_2SQ molecule with respect to the energy of the most stable superstructure.

S1. S. Grimme, *J. Comp. Chem.*, 2006, **27**, 1787.

S2. (a) G. Kresse and J. Hafner, *Phys. Rev. B*, 1993, **47**, 558.; G. Kresse and J. Furthmüller, *Phys. Rev. B*, 1996, **54**, 11169.

S3. G. Kresse and D. Joubert, *Phys. Rev. B*, 1999, **59**, 1758.

S4. C. Rovira, J. J. Novoa and P. Ballone, *J. Chem. Phys.*, 2001, **115**, 6417.

S5. M. J. Frisch, G. W. Trucks, H. B. Schlegel, G. E. Scuseria, M. A. Robb, J. R. Cheeseman, G. Scalmani, V. Barone, B. Mennucci, G. A. Petersson, H. Nakatsuji, M. Caricato, X. Li, H. P. Hratchian, A. F. Izmaylov, J. Bloino, G. Zheng, J. L. Sonnenberg, M. Hada, M. Ehara, K. Toyota, R. Fukuda, J. Hasegawa, M. Ishida, T. Nakajima, Y. Honda, O. Kitao, H. Nakai, T. Vreven, J. A. Montgomery, Jr., J. E. Peralta, F. Ogliaro, M. Bearpark, J. J. Heyd, E. Brothers, K. N. Kudin, V. N. Staroverov, R. Kobayashi, J. Normand, K. Raghavachari, A. Rendell, J. C. Burant, S. S. Iyengar, J. Tomasi, M. Cossi, N. Rega, J. M. Millam, M. Klene, J. E. Knox, J. B. Cross, V. Bakken, C. Adamo, J. Jaramillo, R. Gomperts, R. E. Stratmann, O. Yazyev, A. J. Austin, R. Cammi, C. Pomelli, J. W. Ochterski, R. L. Martin, K. Morokuma, V. G. Zakrzewski, G. A. Voth, P. Salvador, J. J. Dannenberg, S. Dapprich, A. D. Daniels, Ö. Farkas, J. B. Foresman, J. V. Ortiz, J. Cioslowski and D. J. Fox, Gaussian 09, Revision B.1, Gaussian, Inc, Wallingford CT, 2009.

Table S2. Optimized structures and relative energies (in kcal/mol) of five geometric isomers of H_2SQ depending on the position of hydrogen atoms.

a (ZZ) **b (EZ)** **c** **d** **e**

	pure DFT (GGA)					hybrid DFT		
	DFT-D2 (VASP)	DFT-D2 (G09)	BLYP (G09)	PBE (G09)	PW91 (G09)	B3LYP (G09)	PBE0 (G09)	CAM-B3LYP (G09)
a	0.00	0.00	0.00	0.00	0.00	0.00	0.00	0.00
b	2.64	2.56	2.51	2.67	2.65	2.34	2.40	2.16
c	8.56	9.11	8.95	9.27	9.26	8.92	9.10	8.77
d	8.11	8.57	8.74	8.16	8.24	10.34	10.19	12.07
e	8.80	9.21	9.34	8.81	8.88	10.87	10.75	12.60

Figure S2. Initial periodic molecular configurations (1): rectangular grid arrangements in which four-membered carbon rings of H_2SQ are positioned parallel to the unit vectors of the supercell, and the closest distance between the centers of the four-membered carbon rings was set to 6 Å. Supercells are indicated by dashed black lines.

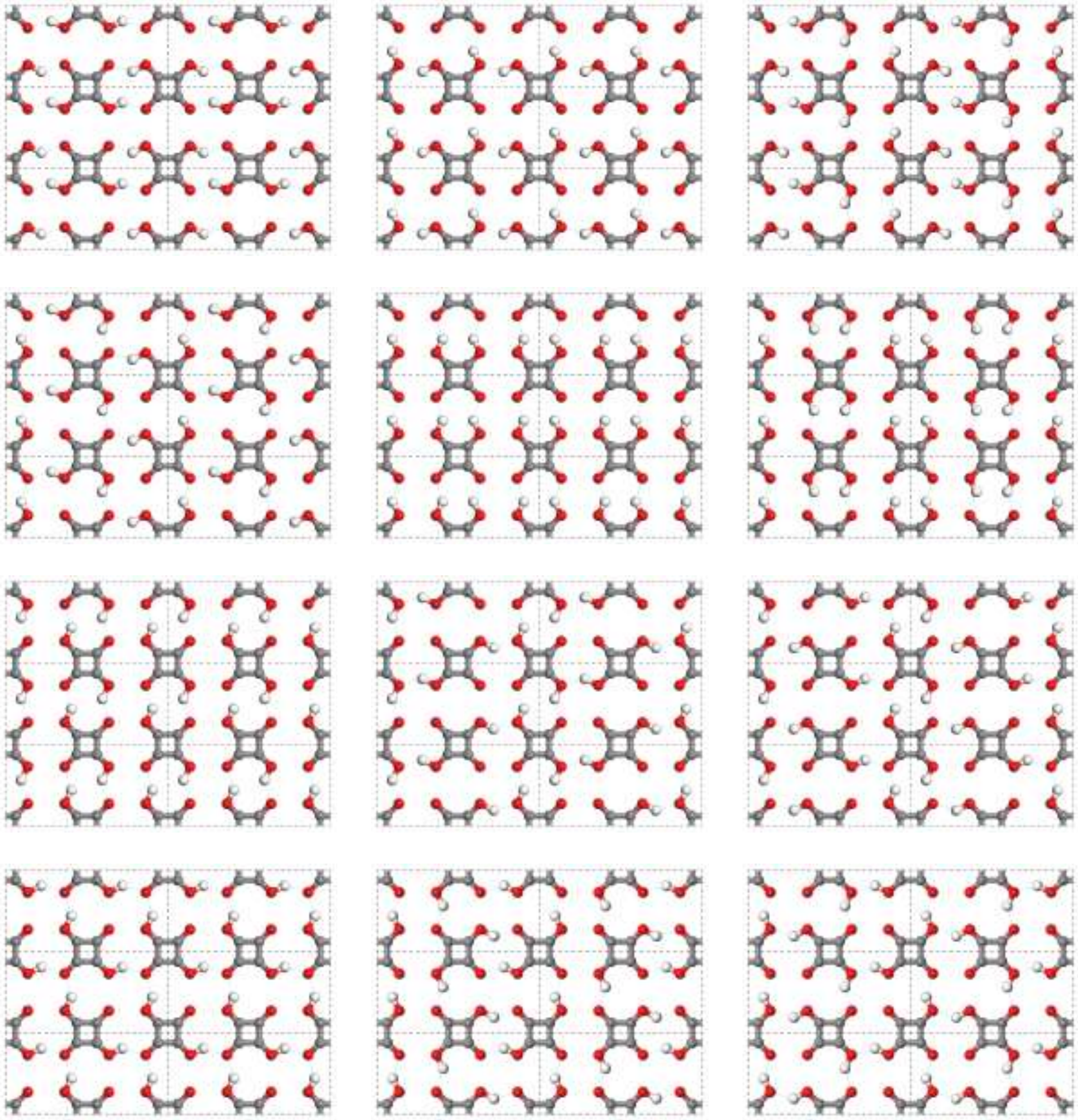

Figure S3. Initial periodic molecular configurations (2): rectangular grid arrangements with the molecules rotating from (1) by anticlockwise 25°. Supercells are indicated by dashed black lines.

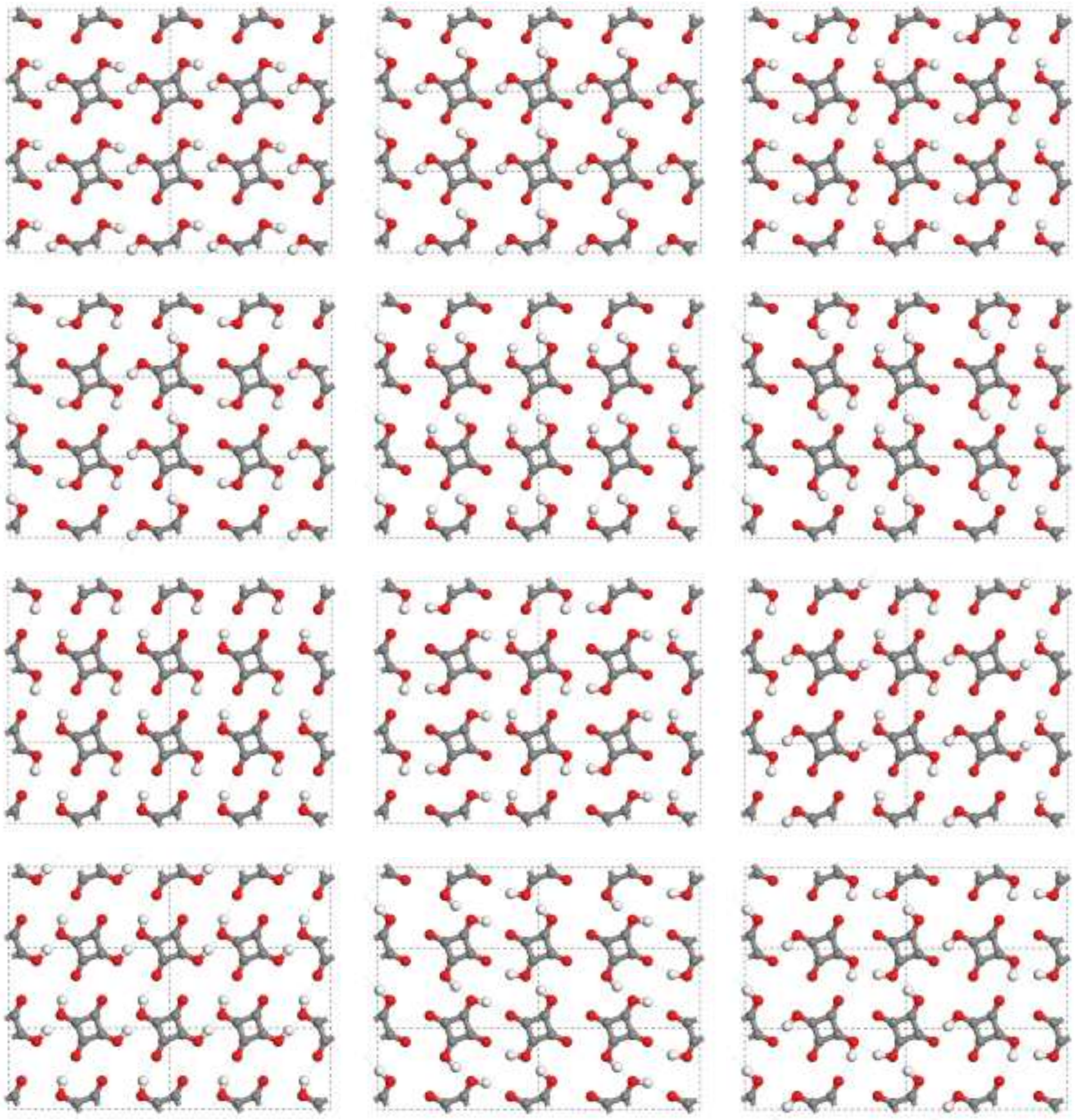

Figure S4. Initial periodic molecular configurations (3): parallelogrammic arrangements tilted from rectangular (1) by ±7°. Supercells are indicated by dashed black lines.

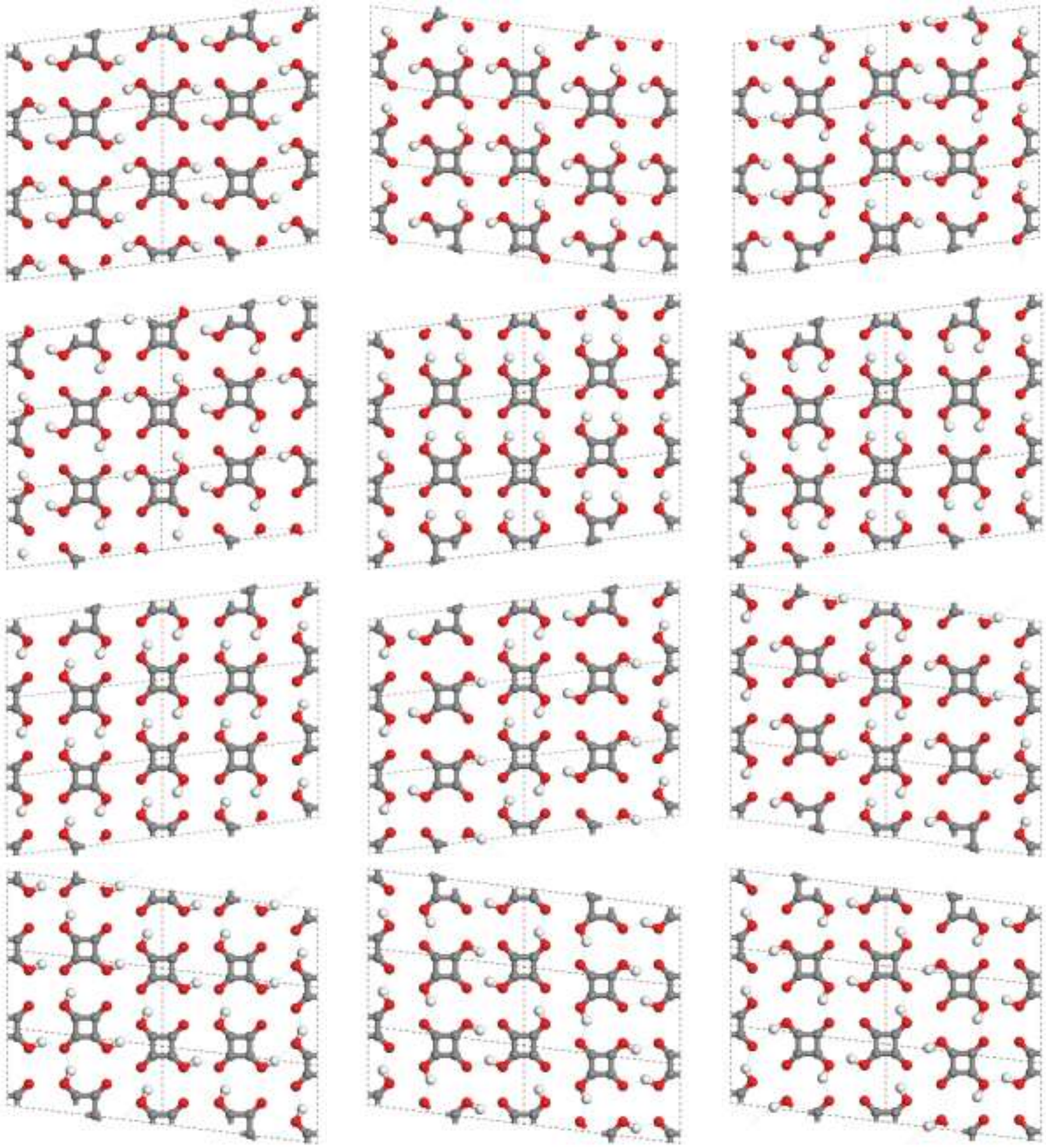

Figure S5. Eight optimized stable superstructures that have relative energies within 10 kcal/mol per H_2SQ molecule with respect to the energy of the most stable superstructure **A**. Numerical values in parentheses are the relative energy (**bold**, in kcal/mol) and binding energy (*italic*, in eV) per one H_2SQ molecule. Binding energy was evaluated with respect to the energy of the most stable isomer **a**, i.e., the **ZZ** isomer, in the gas phase (Table S1), regardless of the isomer species in the optimized periodic molecular configurations. Optimized supercells are indicated by dashed black lines. In particular, two molecules in the unit cell of superstructure **A** have identical geometry, and thus are indistinguishable.

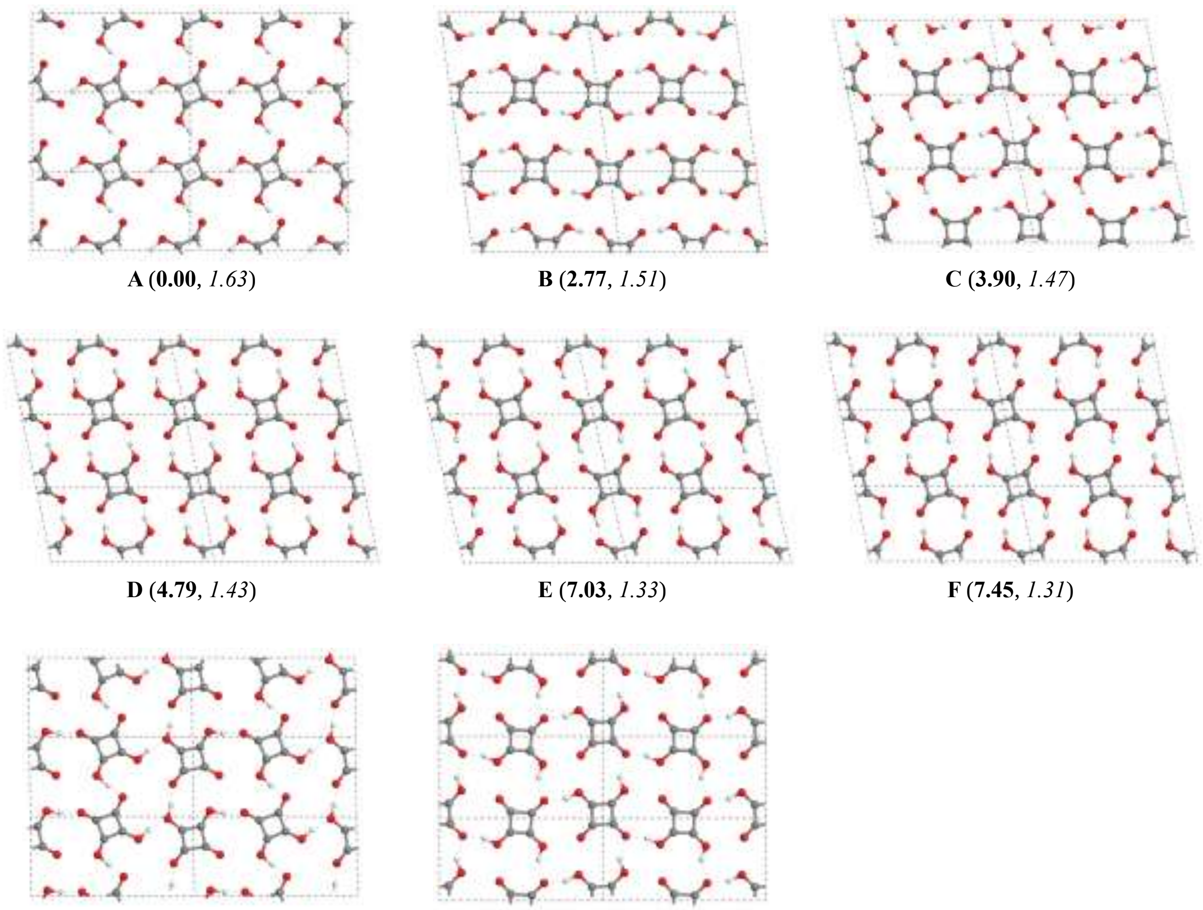

A (**0.00**, *1.63*)

B (**2.77**, *1.51*)

C (**3.90**, *1.47*)

D (**4.79**, *1.43*)

E (**7.03**, *1.33*)

F (**7.45**, *1.31*)

G (**9.34**, *1.23*)

H (**9.46**, *1.22*)

Figure S6. Electron density difference maps for the formation of (a) 1D ribbon and (b) 2D carpet superstructure. Iso-density values are 0.007 *e*/bohr^3, in which the blue (red) region denotes a gain (loss) of electron density during the formation of the molecular array.

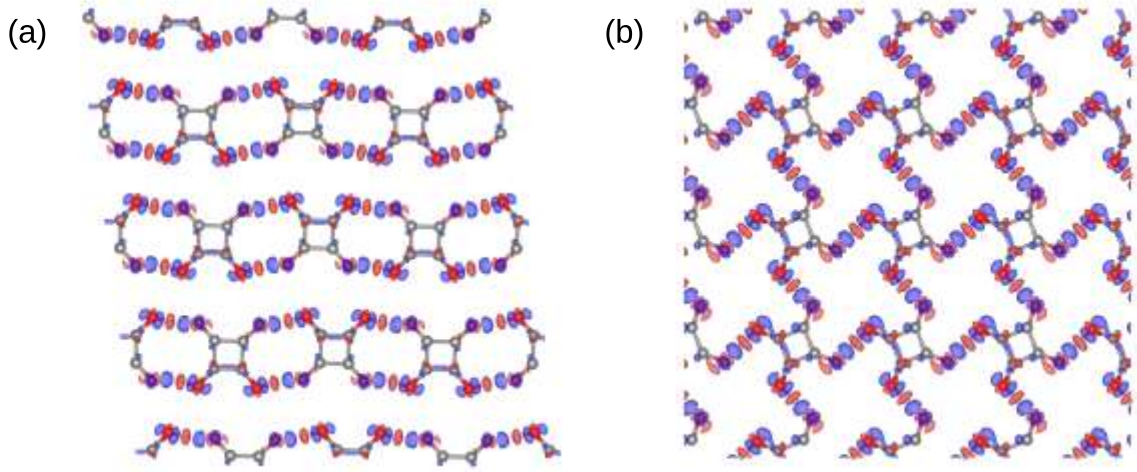

Figure S7. Selected bond lengths (in Å) for (a) 1D ribbon and (b) 2D carpet superstructure. The 2D superstructure shows that the smaller deviation of C-C bond lengths in four-membered ring than that for 1D superstructure, which implies the more highly π-conjugated nature of 2D superstructure compared to 1D superstructure.